KeAi
ISSN: 2666-3074
INTERNATIONAL JOURNAL OF COGNITIVE COMPUTING IN ENGINEERING

KINETIC MODELLING FOR ADSORPTIVE REMOVAL OF ACETIC ACID FROM ITS AQUEOUS SOLUTION USING BIOSORBENTS FROM WASTE BAOBAB AND TAMARIND OF DHOFAR

Sumaya Abdullah Al-Shukaili, Maryam Awadh Al-Shukaili, Hifaa Ali Al-Baraami, Fatema Salim Al-Mamari, Sivamani Selvaraju*

Mechanical and Chemical Engineering Unit, Department of Engineering and Technology, University of Technology and Applied Sciences, Salalah, Oman

Corresponding author - Sivamani Selvaraju

ABSTRACT:

The adsorption kinetics of acetic acid from aqueous solution onto raw and activated baobab (RB, AB) and tamarind (RT, AT) biosorbents of Dhofar were systematically investigated to evaluate the influence of biosorbent activation on adsorption performance and mechanism. Experimental data were analyzed using linear forms of eight kinetic models, including pseudo-first order (PFO), pseudo-second order (PSO), Elovich (EV), Brouers-Sotolongo (BS), Weibull (WB), Hill (HL), intra-particle diffusion (IPD), and Boyd (BY) models. Model performance was assessed through comprehensive error analytical parameters, including sum of squared errors (SSE), mean squared sum of errors (MSSE), standard error (SE), average absolute relative deviation (AARD), determination coefficient (R^2) and correlation coefficient (R), chi-square test (χ^2), and bias (b) factor. Among the adsorption kinetic models, the PSO and BS models demonstrated superior agreement with experimental data for most biosorbents, as evidenced by lower SSE and AARD values, highlighting the dominant chemisorption and heterogeneous adsorption behavior. Diffusion models, such as the IPD and BY models, revealed that adsorption was partly controlled by both boundary layer effects and intra-particle diffusion, with diffusion playing a more significant role in raw biosorbents. Activation of the biosorbents enhanced adsorption capacity and modified the kinetics, suggesting increased availability of active sites and improved surface accessibility. These findings demonstrate that error analysis based on kinetic models provides a robust framework for evaluating adsorption performance and mechanism.

Keywords: Adsorption, Acetic acid, Baobab, Tamarind, Kinetics, Diffusion

INTRODUCTION:

Wastewater is a byproduct of domestic, industrial, and agricultural activities and contains a wide range of physical, chemical, and biological contaminants. If released into the environment without proper treatment, wastewater can severely affect aquatic and terrestrial life [1]. High levels of organic matter consume dissolved oxygen during degradation, leading to oxygen depletion in water bodies, which threatens fish and other aquatic organisms [2]. Toxic substances, nutrients, and pathogens present in wastewater can disrupt ecosystems, spread diseases, and contaminate drinking water sources, ultimately posing risks to human health and food security [3,4].

Organic acids are common constituents of wastewater, especially from food processing, pharmaceutical, textile, and fermentation-based industries. These acids, such as acetic, formic, lactic, and propionic acids, contribute significantly to the chemical oxygen demand (COD) and

biological oxygen demand (BOD) of wastewater[5,6]. High concentrations of organic acids can lower pH levels, making the wastewater corrosive and harmful to biological treatment systems[7]. Acidic conditions may inhibit microbial activity, reduce treatment efficiency, and cause damage to pipes, reactors, and infrastructure. Additionally, organic acids can increase the solubility and mobility of heavy metals, intensifying their toxic effects on living organisms[8,9].

Several treatment methods are used to remove or reduce organic acids in wastewater[7]. Biological treatment processes, such as activated sludge systems and anaerobic digestion, are commonly applied due to their cost-effectiveness and ability to degrade biodegradable organic acids. However, these methods can be sensitive to pH fluctuations and high organic loading rates[10]. Physicochemical methods, including chemical neutralization, membrane filtration, advanced oxidation processes, and adsorption, are also employed, especially when wastewater contains high-strength or non-biodegradable organic acids[11]. The selection of treatment method depends on wastewater characteristics, regulatory standards, and economic considerations[12,13].

Adsorption has gained significant attention as an effective wastewater treatment technique due to its simplicity, flexibility, and high removal efficiency. This method involves the accumulation of pollutants onto the surface of a solid adsorbent, such as activated carbon, biochar, zeolites, or modified natural materials[14,15]. Adsorption is particularly beneficial for treating wastewater with low to moderate concentrations of organic acids and for polishing effluents after biological treatment. It does not produce harmful byproducts, requires relatively simple operation, and can be adapted for different types of contaminants by selecting appropriate adsorbents[16,17]. In this context, the Dhofar region of Oman is rich in naturally abundant and renewable biomass and mineral resources, which remain largely underutilized for environmental applications[18,19]. Utilizing such locally available materials as adsorbents offers a sustainable and cost-effective alternative to commercial products while supporting region-specific wastewater treatment solutions[20-22].

The effectiveness of adsorption processes is strongly influenced by contact time, adsorbent dosage, pollutant concentration, and system conditions. Therefore, kinetic modelling of adsorption plays a crucial role in wastewater treatment design and optimization[23,24]. Kinetic models help describe the rate of adsorption, identify the controlling mechanisms, and predict system performance under different operating conditions[25,26]. Understanding adsorption kinetics allows engineers to design efficient treatment units, minimize costs, and ensure compliance with environmental regulations. Consequently, kinetic modelling is essential for advancing adsorption-based technologies and improving sustainable wastewater treatment practices[27-30].

Recent research demonstrates diverse approaches to acetic acid adsorption across polymeric, environmental, carbonaceous, metallic, and zeolitic systems, highlighting the importance of surface chemistry and intermolecular interactions[31-33]. Polymeric ion-exchange resins have been shown to be highly effective for removing organic acid impurities from non-aqueous solvents[34,35]. Anasthas and Gaikar (2001) reported that styrene–divinylbenzene resins functionalized with tertiary and quaternary amines exhibited high selectivity and adsorption

capacity for acetic acid in ethyl acetate and ethanol. This behavior was attributed to specific hydrogen-bonding interactions between acetic acid and amino groups, underscoring the suitability of ion-exchange resins for solvent purification applications. Also, at environmental interfaces, adsorption of acetic acid on ice has been investigated using combined experimental and molecular simulation methods[36]. Picaud et al. (2005) demonstrated that acetic acid adsorbs on ice predominantly as dimers in the gas phase, with adsorption increasing at lower temperatures. Molecular dynamics simulations revealed that strong surface interactions can dissociate dimers, stabilizing monomeric species on the ice surface. These findings provide mechanistic insights relevant to atmospheric and surface chemistry[37].

Low-cost adsorption strategies have also been explored using agricultural waste–derived activated carbons. Dina et al. (2012) showed that zinc chloride–activated maize cob carbons possess favorable surface properties and adsorption capacities comparable to commercial carbons. Adsorption data fitted multiple isotherm models, confirming favorable sorption and highlighting the role of surface area and pore structure. Moreover, surface science studies have further elucidated acetic acid behavior on metals[38]. Hofman et al. (2020) found that acetic acid adsorbs molecularly on Ni(110) at low temperatures, while higher temperatures promote dissociation to bidentate acetate species and subsequent decomposition. These processes depend strongly on coverage and temperature, with implications for catalytic reactions. Finally, adsorption on acidic zeolites has been examined using spectroscopic and theoretical tools[39] Gomes et al. demonstrated that acetic acid adsorbs molecularly on H-Beta zeolite, primarily via carbonyl interaction with Brønsted acid sites, forming stable complexes relevant to esterification catalysis[40]. Overall, these studies highlight the versatility of adsorption mechanisms for acetic acid and the critical influence of surface functionality, temperature, and molecular configuration across applications.

Although extensive studies have explored the adsorption of organic acids, particularly acetic acid, on diverse materials such as ion-exchange resins, activated carbons, metals, ice surfaces, and zeolites, most existing investigations are either focused on non-aqueous systems, atmospheric or surface chemistry, or catalytic applications rather than realistic wastewater matrices[17,33,39]. Moreover, many adsorption studies emphasize equilibrium behavior and mechanistic surface interactions, with comparatively limited attention given to adsorption kinetics under aqueous, pH-variable, and multicomponent wastewater conditions[34,35]. The dynamic influence of operational parameters on adsorption rates, rate-controlling mechanisms, and process scalability remains insufficiently understood, especially for low-cost or sustainable adsorbents intended for wastewater treatment. Additionally, the integration of kinetic modeling with practical wastewater treatment objectives has not been comprehensively addressed. The novelty of the present study lies in systematically investigating the adsorption kinetics of organic acids in aqueous wastewater systems using an appropriate adsorbent under controlled yet environmentally relevant conditions. By combining experimental adsorption data with kinetic modeling, this work aims to elucidate the dominant mass-transfer and surface-reaction mechanisms governing organic acid removal. Such an approach bridges the gap between fundamental adsorption studies and applied wastewater treatment design, providing insights necessary for optimizing adsorption units and

enhancing process sustainability.

From the above analysis of literature and research gap, the aim of the present study is to remove acetic acid from its aqueous solution using biosorbents prepared from waste baobab and tamarind trees in Dhofar. The objectives are as follows: (i) To prepare raw and activated biosorbents from waste baobab and tamarind trees in Dhofar; (ii) To investigate the effect of time on adsorption capacity for removal of acetic acid from its aqueous solution using raw and activated biosorbents from waste baobab and tamarind trees in Dhofar; and (iii) To analyze mechanistic kinetic models, pseudo-first order (Lagergren), pseudo-second order, Elovich, Brouers-Sotolongo, Weibull, Hill, Boyd, and intra-particle diffusion models, for adsorption of acetic acid on biosorbents.

MATERIALS AND METHODS:

Materials:

All chemicals used were of analytical grade and employed without further purification. Glacial acetic acid (≥99%, Sigma-Aldrich) was used to prepare the adsorbate solutions. Distilled water was used for all solution preparations and washing steps. Raw and activated biosorbents were prepared from locally sourced materials of Dhofar.

Preparation of adsorbate:

A 1.0 M acetic acid stock solution was prepared by diluting analytical-grade glacial acetic acid with distilled water. Specifically, 28.5 mL of acetic acid was accurately measured using a calibrated volumetric pipette and transferred into a 500 mL volumetric flask. Distilled water was then added gradually to the flask until the final volume reached 500 mL, corresponding to a total of 471.5 mL of water. The solution was thoroughly mixed to ensure homogeneity and subsequently used as the adsorbate for all adsorption experiments. Required working solutions of lower concentrations were prepared by appropriate dilution of the stock solution with distilled water prior to use.

Preparation of raw and activated baobab and tamarind biosorbents:

Raw biosorbents were prepared from dried leaves of baobab (*Adansonia digitata*) and tamarind (*Tamarindus indica*) of Dhofar collected from Wadi Hanna and Taqah, respectively, in Dhofar governorate, Oman. The collected leaves were first air-cleaned separately to remove adhering dust and surface impurities and subsequently sun-dried for five days to ensure complete moisture removal. After drying, unwanted materials such as petioles, bark fragments, and other foreign matter were manually removed[20,41]. The cleaned leaves were ground using a domestic blender to obtain fine powder. The ground materials were sieved through a 1.0 mm mesh screen, and the fractions passing through the sieve were collected as raw biosorbents and stored in airtight containers for further use. The coarse fractions retained on the sieve were discarded.

Chemical activation of both raw biosorbents was carried out using sulfuric acid. For each material, 25 g of the raw biosorbent powder was mixed with 75 mL of 4.0 M sulfuric acid to form a homogeneous paste. The mixture was allowed to stand for 1 h to facilitate chemical activation[42]. Following activation, the biosorbents were thoroughly washed with distilled water

until the washings were free of excess acid. The washed materials were then sun-dried for five days to ensure complete removal of moisture. After drying, the final masses of the activated baobab and tamarind biosorbents were recorded and the materials were used in subsequent adsorption experiments. The yield of each activated biosorbent was calculated as the ratio of the final dried mass to the initial mass of the corresponding raw biosorbent, as given in Equation (1).

$$\text{Yield } \% = \frac{Mass\ of\ activated\ biosorbent}{Mass\ of\ raw\ powder} \times 100 \quad (1)$$

Effect of contact time on adsorption capacity for acetic acid removal from its aqueous solution using raw and activated baobab and tamarind biosorbents:

Batch adsorption experiments were conducted to investigate the effect of contact time on the removal of acetic acid using raw and activated baobab and tamarind biosorbents. Standard solutions of acetic acid were prepared by diluting their 1.0 M stock solutions with distilled water to obtain the desired concentrations in 50 mL aliquots placed in four separate 250 mL conical flasks[43]. A fixed mass of biosorbent (0.1 g) was added to each flask, corresponding to raw baobab (RB), activated baobab (AB), raw tamarind (RT), and activated tamarind (AT) biosorbents. The mixtures were agitated on a magnetic stirrer at 150 rpm at room temperature (~25 °C) for predetermined time intervals. At each time interval of 2 min, 10 mL of the supernatant was withdrawn, filtered through Whatman No. 42 filter paper to remove suspended biosorbent particles, and analyzed for residual acetic acid concentration using a UV–Vis spectrophotometer at 210 nm. The experiments were repeated until equilibrium was reached, as indicated by no significant change in the measured concentration of acids. All measurements were performed in triplicate to ensure reproducibility. The residual concentrations obtained from UV–Vis analysis were used to calculate the adsorption capacity at any time t (q_t), as given in Equation (2).

$$q_t = \frac{(C_0 - C_t)\,V}{m} \quad (2)$$

where, C_0 and C_t are the initial and time-dependent concentrations of the acid (mol.L^{-1}), V is the volume of the solution (L), and m is the mass of the biosorbent (g). This procedure allowed systematic evaluation of the adsorption kinetics and comparison of the performance of raw versus activated biosorbents. Kinetic studies were performed by monitoring the change in acetic acid concentration at various contact times.

Analytical method for residual acetic acid in aqueous solution:

The residual concentration of acetic acid in aqueous solutions after adsorption was determined using a UV–Vis spectrophotometer (Model: UV-1800, Shimadzu) at a wavelength of 210 nm, which corresponds to the characteristic absorption of the carboxyl group. Prior to analysis, samples were filtered through Whatman No. 42 filter paper to remove any suspended biosorbent particles[44]. A calibration curve was prepared using standard acetic acid solutions of known concentrations ranging from 0.1 to 1.0 M. Each standard solution was measured in triplicate, and the absorbance was plotted against concentration to obtain a linear calibration curve with a correlation coefficient (R^2) above 0.995. Sample absorbances were then measured under identical conditions, and their concentrations were determined from the calibration curve. All measurements were conducted at room temperature (~25 °C). For quality control, blank samples

containing only distilled water were analyzed to account for baseline absorbance, and all readings were corrected accordingly.

Kinetic models used in the adsorption of acetic acid from its aqueous solution using raw and activated biosorbents from waste baobab and tamarind trees in Dhofar:

Pseudo-first order (PFO) model

The pseudo-first order (Lagergren) kinetic model assumes that the adsorption rate is proportional to the number of unoccupied sites on the biosorbent surface and is mainly applicable to physical adsorption at the initial stage, as shown in Equation (3):

$$\log(q_e - q_t) = \log q_e - \left(\frac{K_1}{2.303}\right) t \quad (3)$$

where, q_e is equilibrium adsorption capacity (mol.g^{-1}), K_1 is pseudo-first order rate constant (min^{-1}), and t is time (min)[35].

Pseudo-Second order model

The pseudo-second-order kinetic model assumes that the adsorption rate is controlled by chemical interactions between the adsorbate and the biosorbent and depends on the availability of active sites, as shown in Equation (4):

$$\frac{t}{q_t} = \frac{1}{K_2 {q_e}^2} + \frac{1}{q_e}\, t \quad (4)$$

where, K_2 is pseudo-second order rate constant (mol^{-1}.g^{-1}.min^{-1})[35].

Elovich model

The Elovich model is used to describe adsorption processes on energetically heterogeneous surfaces where the activation energies vary for different adsorption sites. The model is represented by Equation (5):

$$q_t = \frac{ln(\alpha\beta)}{\beta} + \frac{ln\, t}{\beta} \quad (5)$$

$$\ln t = q_t\beta - ln(\alpha\beta)$$

where, α is initial adsorbate adsorption rate (mol·g^{-1}·min^{-1}), β is adsorption constant (g·mol^{-1}), Initial adsorption rate (α) and adsorption constant (β) can be evaluated from a linear plot of qt versus ln t[35].

Brouers-Sotolongo fractal kinetic model

The Brouers-Sotolongo fractal kinetic model is used to describe adsorption processes occurring on heterogeneous surfaces, such as nanomaterials, where complex geometric and energetic factors influence sorption kinetics. The model is expressed as shown in Equation (6):

$$q_t = q_e(1 - \exp(-kt)^a) \quad (6)$$

where, n is apparent reaction order, k is rate constant (min^{-1}), a is global fractal time index due to supposed fractal diffusion and sorption kinetics arising from geometric and energetic heterogeneity of adsorbent[45,46].

Weibull kinetic model

The Weibull kinetic model is commonly used to describe adsorption processes on heterogeneous

surfaces and systems with complex sorption kinetics. The model is expressed as shown in Equation (7):

$$q_t = q_e\left(1 - \exp\left(-\frac{t}{\tau}\right)^a\right) \quad (7)$$

where $\tau_{50\%} = \tau(\ln 2)^{1/a}$, $\tau_{50\%}$ represents the time required to adsorb one-half of the maximum adsorbed quantity[47].

Hill kinetic model

The Hill kinetic model describes adsorption processes on heterogeneous surfaces, particularly when cooperative effects influence the rate of adsorption, as shown in Equation (8):

$$q_t = q_e\left(\frac{(t/\tau)^a}{1+(t/\tau)^a}\right) \quad (8)$$

where, $\tau = (k_{2,aq_m})^{-1/a}$ and $\tau_{50\%} = \tau$[47].

Intra-particle diffusion model:

The intra-particle diffusion model (Weber-Morris model) is used to identify whether diffusion within the pores of the adsorbent is the rate-limiting step in the adsorption process. The model is expressed in Equation (9) as:

$$q_t = K_{IPD}\, t^{1/2} + C \quad (9)$$

where K_{IPD} is intra-particle diffusion constant (mol·g^{-1}.min$^{-1/2}$), C = Thickness of boundary layer (mol.g^{-1})[47].

Boyd model

The Boyd model is used to determine the rate-controlling step in adsorption processes, distinguishing whether external mass transfer or internal diffusion is the slow step, as shown in Equation (10):

$$B_t = Bt = -0.4977 - \ln\left(1 - \frac{q_t}{q_e}\right) \quad (10)$$

where B is Boyd rate constant[47].

Error analytical parameters for kinetic modelling of adsorption of acetic acid using raw and activated baobab and tamarind biosorbents:

In kinetic modelling of adsorption processes, statistical error analysis is essential to evaluate the adequacy, reliability, and predictive capability of proposed kinetic models. For the adsorption of acetic acid onto raw and activated baobab and tamarind biosorbents, error analytical parameters are used to quantify the deviation between experimentally observed values and model-predicted values. These parameters provide insight into goodness-of-fit, model accuracy, and consistency, thereby supporting the selection of the most appropriate kinetic model[48,49].

Residual or error sum of squares (absolute)

Residual or error sum of squares (SSE), as given in Equation (11), measures the total squared deviation between experimental observations and model predictions. It directly reflects the overall discrepancy of the kinetic model from experimental data. Lower SSE values indicate a better fit of the kinetic model to experimental adsorption data.

$$SSE = \sum_{i=1}^{n}(Y_o - Y_p)^2 \quad (11)$$

where Y_o and Y_p are experimental and predicted values of adsorption capacity[49].

Error variance of the estimate (MSSE)

Error variance of the estimate (MSSE), as given in Equation (12), represents the average squared error per degree of freedom and accounts for the number of fitted parameters in the model. It provides a normalized measure of model error. Smaller MSSE values signify higher model precision and reliability.

$$MSSE = \frac{SSE}{n-p} \quad (12)$$

where n is number of experimental data considered for analysis, and p is number of model parameters[49].

Standard error of the estimate (SE)

Standard error of the estimate (SE), as given in Equation (13), indicates the dispersion of experimental data points around the predicted values and is expressed in the same units as the response variable. Lower SE values suggest closer agreement between experimental and predicted adsorption kinetics[49].

$$SE = \sqrt{\frac{SSE}{n-p}} \quad (13)$$

Absolute average deviation (AARD)

Absolute average deviation (AARD), as given in Equation (14), evaluates the average relative deviation between experimental and predicted values, making it particularly useful for comparing models across different data scales. Lower AARD values (typically < 10%) indicate excellent model performance[49].

$$Absolute\ average\ deviation\ AARD = \frac{1}{n}\sum_{i=1}^{n}\frac{|Y_o - Y_p|}{Y_o} \quad (14)$$

Determination coefficient (R^2)

Determination coefficient (R^2), as given in Equation (15), quantifies the proportion of variance in the experimental data explained by the kinetic model. It is a primary indicator of goodness-of-fit. R^2 values closer to 1 indicate superior model accuracy[49].

$$Determination\ coefficient\ R^2 = \frac{\sum_{i=1}^{n}(Y_p - \bar{Y}_p)^2}{\sum_{i=1}^{n}(Y_p - \bar{Y}_p)^2 + \sum_{i=1}^{n}(Y_o - Y)^2} \quad (15)$$

Correlation coefficient (R)

Correlation coefficient (R), as given in Equation (16), measures the strength of the linear relationship between experimental and predicted adsorption data. R values approaching unity indicate strong correlation and good predictive capability[49].

$$Correlation\ coefficient\ R = \sqrt{\frac{\sum_{i=1}^{n}(Y_p - \bar{Y}_p)^2}{\sum_{i=1}^{n}(Y_p - \bar{Y}_p)^2 + \sum_{i=1}^{n}(Y_o - Y)^2}} \quad (16)$$

Chi-square (χ^2) test

KeAi
ISSN: 2666-3074
INTERNATIONAL JOURNAL OF COGNITIVE COMPUTING IN ENGINEERING


The chi-square (χ^2), as given in Equation (17), test evaluates the statistical significance of the difference between observed and predicted values, weighted by the experimental values. Lower χ^2 values indicate minimal deviation and a better fit between the kinetic model and experimental data[49].

$$Chi - square\ \chi^2 = \frac{\sum_{i=1}^{n}(O_i - E_i)^2}{E_i} \quad (17)$$

Bias

Bias), as given in Equation (18), assesses the systematic tendency of a model to overpredict or underpredict experimental adsorption data. A bias value close to 1 indicates negligible systematic error and unbiased model predictions[49].

$$Bias\ b = exp(\frac{1}{n}\sum_{i=1}^{n} \ln\ (\frac{Y_o}{Y_P})) \quad (18)$$

RESULTS AND DISCUSSION:

Biosorbent yield:

Table 1. Yield of activated biosorbents from raw powder for baobab and tamarind

Source of biosorbent	Mass of raw powder (g)	Mass of activated biosorbent (g)	Yield (%)
Baobab	25	11.11	44.44
Tamarind	25	14.00	56.00

Table 1 shows the yield of activated biosorbents derived from two sources: Baobab and Tamarind. Yield represents the efficiency of converting raw biosorbent into its activated form, quantified as a percentage of the total mass of the original raw material used. The data indicates that for every 25 grams of raw baobab powder, 11.11 grams of activated biosorbent were produced, resulting in a yield of 44.44%. The yield shows moderate efficiency of conversion from raw powder to activated biosorbent. Similarly, for tamarind, 25 grams of raw powder resulted in 14.00 grams of activated biosorbent, giving 56% yield. Tamarind is a more efficient biosorbent source, yielding a higher percentage of activated material compared to baobab.

Effect of contact time on adsorption capacity for acetic acid removal from its aqueous solution using raw and activated biosorbents from waste baobab and tamarind trees:

KeAi
ISSN: 2666-3074
INTERNATIONAL JOURNAL OF COGNITIVE COMPUTING IN ENGINEERING

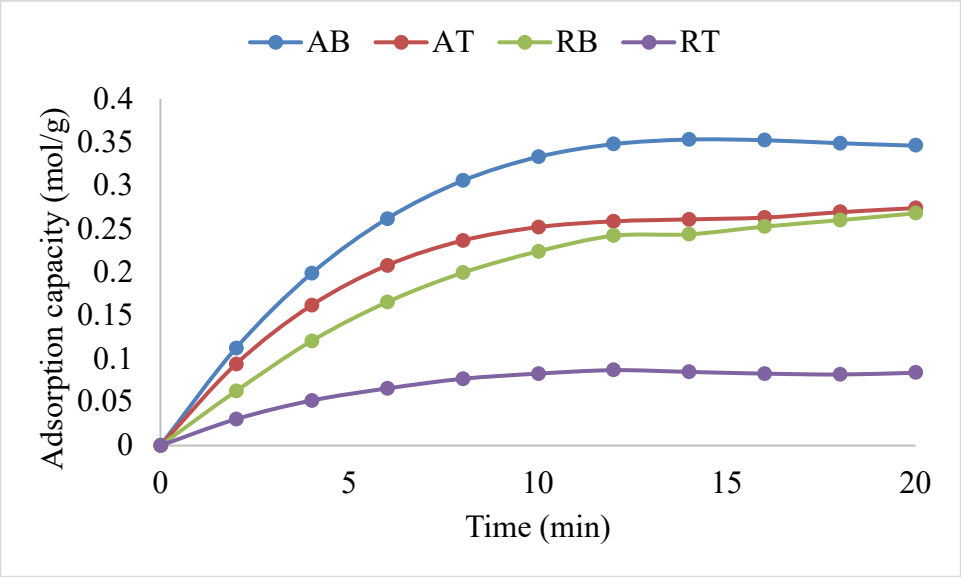

Figure 1. Effect of contact time on adsorption capacity for acetic acid removal from its aqueous solution using raw and activated biosorbents from waste baobab and tamarind trees (AB: Activated baobab, AT: Activated tamarind, RB: Raw baobab, RT: Raw tamarind)

Figure 1 shows the effect of time on adsorption capacity of raw and activated baobab and tamarind biosorbents for removal of acetic acid from its aqueous solution. Adsorption capacity increases gradually with the contact time. After 2 min, the capacity increases to 0.112, 0.094, 0.063, and 0.030 mol/g, respectively, for AB, AT, RB and RT, indicating that the biosorbent quickly starts to capture acetic acid within the first few minutes, and further increasing to 0.333, 0.252, 0.224, and 0.083 mol/g, respectively, at 10 min[20]. As time continues, from 10 to 20 min, the adsorption capacity reaches equilibrium during this period at 0.353, 0.259, 0.244, and 0.087 mol/g, respectively, at 14, 12, 14, and 12 min, for AB, AT, RB, and RT. The initial rapid increase means that the biosorbent is very effective at adsorbing acetic acid in the early stages. After about 10 min, the increase slows down, suggesting that most of the available adsorption sites are filled. The biosorbents are effective in removing acetic acid in the order of AB>AT>RB>RT. The more rapid adsorption of acetic acid by baobab biosorbents compared to tamarind is likely due to higher surface area, greater porosity, and a larger number of accessible functional groups on baobab, which provide more active sites for binding acetic acid molecules. Additionally, the chemical composition of baobab, rich in hydroxyl and carboxyl groups, enhances interactions with acetic acid through hydrogen bonding and electrostatic attraction, resulting in faster uptake and higher adsorption capacity relative to tamarind[21].

Kinetic models used in the adsorption of acetic acid using raw and activated baobab and tamarind biosorbents:

Table 2 shows the kinetic model parameters for the adsorption of acetic acid onto raw and activated baobab and tamarind biosorbents, obtained by fitting the experimental data to various kinetic and diffusion models. Kinetic modeling is an essential tool for understanding the adsorption mechanism, adsorption rate, and rate-controlling steps of pollutants onto biosorbents.

In this study, the adsorption behavior of acetic acid was analyzed using pseudo-first-order (PFO) and pseudo-second-order (PSO) models to determine whether physisorption or chemisorption governs the process. The Elovich (EV) model was applied to describe adsorption on energetically heterogeneous surfaces, while the Brouers–Sotolongo (BS) and Weibull (WB) models were used to account for surface heterogeneity and fractal-like adsorption kinetics. The Hill (HL) model provided insight into cooperative adsorption behavior among active sites. In addition, the intraparticle diffusion (IPD) and Boyd (BY) models were employed to evaluate the contribution of pore diffusion and boundary layer resistance to the overall adsorption rate. The combined application of these models enables a comprehensive understanding of the adsorption mechanism, kinetic efficiency, and the effect of biosorbent activation on acetic acid removal.

Table 2. Model parameters in the adsorption kinetics of acetic acid using raw and activated baobab and tamarind biosorbents

Model	Parameters	AB	AT	RB	RT
PFO	K_1 (min^{-1})	0.6798	0.6893	0.4756	0.9164
	q_e (mol/g)	0.4258	0.3053	0.2858	0.1234
PSO	K_2 ($mol.L^{-1}min^{-1}$)	2.0077	1.3487	3.5491	0.3341
	q_e (mol/g)	0.4475	0.3347	0.3981	0.1013
EV	α ($mol·g^{-1}·min^{-1}$)	8.7575	12.215	10.751	41.330
	β ($g·mol^{-1}$)	0.1077	0.0773	0.0920	0.0237
BS	a	1.2799	1.2652	1.3449	1.2454
	k (min^{-1})	0.1625	0.1878	0.1259	0.1826
WB	a	1.2799	1.2652	1.3449	1.2454
	τ (min)	6.1538	5.3248	7.9428	5.4764
HL	τ (min)	2.9700	2.7300	3.3500	2.8200
	a	2.1300	2.2300	2.0900	2.1400
IPD	K_{IPD} ($mol·g^{-1}.min^{-1/2}$)	0.0839	0.0628	0.0649	0.0196
	C ($mol.g^{-1}$)	0.0265	0.0257	0.0021	0.0097
BY	B (min^{-1})	0.2045	0.2153	0.1300	0.2809

The PFO rate constant (k_1) represents the rate of adsorption governed primarily by physical interaction and external mass transfer. The relatively higher k_1 value for RT indicates a faster initial uptake of acetic acid, while lower values for RB suggest slower surface interaction. However, PFO alone does not adequately describe the entire adsorption process, as it generally underestimates equilibrium adsorption capacity.

The PSO rate constant (k_2) and calculated equilibrium adsorption capacity (q_e) indicate that chemisorption is the dominant rate-controlling mechanism. The higher k_2 values for RB and AB suggest stronger adsorbate–adsorbent interactions. The good agreement of q_e values confirms that adsorption proceeds mainly through electron sharing or exchange between acetic acid and surface functional groups.

The Elovich parameters α (initial adsorption rate) and β (desorption constant related to surface heterogeneity) indicate multilayer adsorption on energetically heterogeneous surfaces. Higher α values, especially for RT, reflect rapid initial adsorption, whereas lower β values indicate stronger surface binding and lower desorption tendency.

The BS model describes adsorption kinetics on highly heterogeneous and fractal surfaces. The parameter a represents the fractal time exponent related to surface heterogeneity, while the rate constant k reflects adsorption intensity. Comparable a values across biosorbents indicate similar heterogeneity, while higher k values for AT and RT suggest enhanced adsorption rates due to surface activation or pore accessibility.

In the Weibull model, the shape parameter a characterizes the distribution of adsorption sites, while the scale parameter τ represents the characteristic adsorption time. Lower τ values for AT and RT indicate faster adsorption kinetics, confirming improved surface reactivity and mass transfer compared to raw biosorbents.

The Hill constant (τ) reflects the time required to reach half of the adsorption capacity, while the Hill coefficient (a) indicates cooperative adsorption behavior. Values of a>1 for all biosorbents suggest positive cooperativity, implying that adsorption of acetic acid molecules enhances subsequent adsorption on neighboring sites.

The intraparticle diffusion coefficient (K_{IPD}) quantifies the diffusion rate of acetic acid within biosorbent pores, while the intercept C indicates boundary layer thickness. The non-zero C values for all biosorbents confirm that intraparticle diffusion is not the sole rate-limiting step and that film diffusion contributes significantly to adsorption kinetics.

The Boyd constant (B) is used to distinguish between film diffusion and particle diffusion control. Higher B values for RT and AT indicate faster mass transfer, suggesting that film diffusion dominates the initial adsorption stage, followed by intraparticle diffusion at later stages.

Considering each adsorbent, Adsorption of acetic acid on AB is dominated by chemisorption on a heterogeneous surface, as supported by PSO, Elovich, BS, and Hill models. Diffusion effects contribute but do not control the overall rate. AT exhibits rapid adsorption kinetics and strong chemisorptive interaction, with lower Weibull characteristic times and higher Brouers–Sotolongo rate constants. The mechanism involves surface-controlled adsorption enhanced by activation-induced porosity. RB shows chemisorption with significant intraparticle diffusion resistance, indicated by lower diffusion constants and higher characteristic times. The adsorption process is governed by mixed control involving surface reaction and pore diffusion. RT demonstrates fast initial uptake but lower equilibrium capacity, suggesting film diffusion–assisted chemisorption. Higher Elovich α and Boyd B values indicate strong surface activity with diffusion limitations due to lack of activation.

The kinetic analysis confirms that chemisorption on heterogeneous surfaces is the primary

mechanism for acetic acid adsorption across all biosorbents, while film diffusion and intraparticle diffusion act as secondary controlling steps. Activation significantly enhances adsorption rate, surface heterogeneity, and mass transfer efficiency.

Error analytical parameters for kinetic modelling of adsorption of acetic acid using raw and activated baobab and tamarind biosorbents:

Error analysis is essential for evaluating the adequacy of kinetic models in describing acetic acid biosorption onto raw and activated baobab and tamarind biosorbents (AB, AT, RB, and RT). Statistical error functions such as SSE, MSSE, SE, AARD, χ^2, together with correlation indicators (R^2 and R), were employed to assess the goodness of fit and predictive reliability of different kinetic models (Table 3). Models with lower error values and higher correlation coefficients are considered more suitable for describing the experimental data.

Table 3. Error analytical parameters in kinetic modeling of acetic acid using raw and activated baobab and tamarind biosorbents

Model	Error parameters	AB	AT	RB	RT
PFO	SSE	0.2094	0.1027	0.2943	0.0088
	MSSE	0.0233	0.0114	0.0327	0.0010
	SE	0.1525	0.1068	0.1808	0.0313
	AARD	0.5963	0.5234	1.0527	0.4816
	R^2	0.9712	0.9887	0.9857	0.9184
	R	0.9855	0.9943	0.9928	0.9583
	χ^2	0.5146	0.3368	0.8218	0.0935
	b	0.6530	0.6776	0.5117	0.7043
PSO	SSE	0.1031	0.0134	0.2680	0.0230
	MSSE	0.0115	0.0015	0.0298	0.0026
	SE	0.1070	0.0386	0.1726	0.0506
	AARD	0.4246	0.1916	1.0640	0.6603
	R^2	0.9759	0.9907	0.9759	0.9774
	R	0.9879	0.9953	0.9879	0.9886
	χ^2	0.2959	0.0627	0.7721	0.9859
	b	0.7255	0.8473	0.5225	3.0573
EV	SSE	0.1563	0.0581	0.2812	0.0159
	MSSE	0.0174	0.0065	0.0313	0.0018
	SE	0.1298	0.0727	0.1767	0.0410
	AARD	0.5105	0.3575	1.0584	0.5710
	R^2	0.9736	0.9897	0.9808	0.9479
	R	0.9867	0.9948	0.9904	0.9736
	χ^2	0.4053	0.1998	0.7970	0.5397
	b	0.6893	0.7625	0.5171	1.8808
BS	SSE	0.0355	0.0227	0.0693	0.0011

	MSSE	0.0039	0.0025	0.0077	0.0001
	SE	0.0628	0.0503	0.0877	0.0113
	AARD	0.1590	0.1734	0.3099	0.1201
	R^2	0.9941	0.9952	0.9954	0.9919
	R	0.9970	0.9976	0.9977	0.9959
	χ^2	0.0863	0.0726	0.1998	0.0124
	b	0.8944	0.8718	0.7811	0.9320
WB	SSE	0.0355	0.0227	0.0693	0.0011
	MSSE	0.0039	0.0025	0.0077	0.0001
	SE	0.0628	0.0503	0.0877	0.0113
	AARD	0.1590	0.1734	0.3099	0.1201
	R^2	0.9941	0.9952	0.9954	0.9919
	R	0.9970	0.9976	0.9977	0.9959
	χ^2	0.0863	0.0726	0.1998	0.0124
	b	0.8944	0.8718	0.7811	0.9320
HL	SSE	0.0719	0.0403	0.1571	0.0021
	MSSE	0.0080	0.0045	0.0175	0.0002
	SE	0.0894	0.0669	0.1321	0.0151
	AARD	0.2844	0.2743	0.6292	0.1889
	R^2	0.9604	0.9595	0.9665	0.9520
	R	0.9800	0.9795	0.9831	0.9757
	χ^2	0.1852	0.1355	0.4653	0.0231
	b	0.7801	0.7861	0.6165	0.8424
IPD	SSE	0.0115	0.3134	0.3244	0.0346
	MSSE	0.0011	0.0285	0.0295	0.0032
	SE	0.0324	0.1688	0.1717	0.0561
	AARD	0.1095	0.7214	0.8189	0.8531
	R^2	0.9175	0.9243	0.9673	0.8858
	R	0.9579	0.9614	0.9835	0.9412
	χ^2	1	0.8839	0.5017	0.9687
	b	1	3.7000	5.7900	6.8500
BY	SSE	0.0396	0.1255	0.1836	0.0126
	MSSE	0.0043	0.0118	0.0182	0.0012
	SE	0.0615	0.0953	0.1305	0.0275
	AARD	0.1843	0.3897	0.5860	0.3874
	R^2	0.9573	0.9597	0.9764	0.9432
	R	0.9784	0.9796	0.9881	0.9712
	χ^2	0.4238	0.3640	0.3889	0.3347
	b	0.8915	1.7860	2.3959	2.8748

The PFO model shows moderate performance across all biosorbents. Although relatively high R^2 and R values (generally >0.91) indicate acceptable correlation with experimental data, the

comparatively larger SSE, MSSE, AARD, and χ^2 values—particularly for raw biosorbents—suggest noticeable deviations between predicted and experimental uptake. This indicates that the PFO model is less capable of accurately describing the overall sorption kinetics, especially during later stages of adsorption.

The PSO model demonstrates improved fitting compared to PFO, with lower SSE, MSSE, SE, and AARD values for most biosorbents, particularly the activated forms. High R^2 (≈0.97–0.99) and R values confirm a strong agreement between predicted and experimental data. The reduced χ^2 values further indicate that the PSO model effectively captures the adsorption kinetics, implying that chemisorption mechanisms may dominate the acetic acid uptake process.

The EV model presents moderate predictive ability. While R^2 values remain relatively high, the error indicators (SSE, AARD, and χ^2) are higher than those observed for PSO and BS models. This suggests that although the EV model can describe heterogeneous surface adsorption, it does not fully represent the kinetic behavior of acetic acid biosorption on these materials.

The BS model exhibits excellent performance across all biosorbents. It records very low SSE, MSSE, SE, AARD, and χ^2 values alongside the highest R^2 and R values (≈0.99). These results indicate minimal deviation between experimental and predicted data, highlighting the strong suitability of the BS model in explaining pore diffusion-controlled adsorption of acetic acid on both raw and activated biosorbents.

The WB model shows statistical results identical to the BS model in this dataset, with very low error values and very high correlation coefficients. This confirms the significant role of intraparticle diffusion in the biosorption process. However, despite its good fit, WB alone may not fully describe the entire kinetic mechanism, as boundary layer effects are not explicitly captured.

The HL model demonstrates moderate accuracy. Although correlation coefficients are reasonably high, the higher error parameters compared to BS and PSO models indicate less precise predictions. This suggests that diffusion-controlled assumptions of the HL model are only partially applicable to the biosorption system studied.

The IPD model shows relatively high SSE, AARD, and χ^2 values, particularly for activated biosorbents, despite acceptable R^2 values. This indicates that intraparticle diffusion is involved but is not the sole rate-controlling step in the adsorption process, limiting the predictive accuracy of this model when used independently.

The Boyd model yields low to moderate error values and reasonable correlation coefficients. However, higher χ^2 and AARD values compared to BS and PSO models suggest that film diffusion is not the dominant controlling mechanism throughout the adsorption process.

Overall, the BS and WB models exhibit the best predictive performance, characterized by the

lowest error values and highest correlation coefficients, indicating excellent agreement with experimental data. The PSO model also shows strong predictive capability and reliably describes the adsorption kinetics. In contrast, PFO, EV, HL, IPD, and Boyd models display comparatively higher errors, suggesting limited applicability or partial control of the adsorption mechanism. Consequently, BS and PSO models are identified as the most reliable for predicting acetic acid biosorption behavior on raw and activated baobab and tamarind biosorbents.

CONCLUSION:

Kinetic analysis of acetic acid adsorption onto raw and activated baobab and tamarind biosorbents has been executed. Activated biosorbents exhibited higher adsorption capacities and faster kinetics, highlighting the positive effect of activation on exposing additional active sites and enhancing surface accessibility. Among the kinetic models, the pseudo-second order and Brouers-Sotolongo models provided the best fit for most biosorbents, indicating that chemisorption and surface heterogeneity govern the adsorption process. Diffusion models, including intra-particle diffusion and Boyd models, showed that both boundary layer effects and diffusion contribute to the rate-limiting step, with diffusion being more pronounced in raw biosorbents. The current analysis relied on reported kinetic parameters, and the study did not quantify the number, distribution, or specific chemical nature of active sites. Further investigations should include site-specific modeling that explicitly accounts for the number and affinity of active sites, as well as adsorption under varying pH, temperature, agitation speed, and multicomponent systems. Incorporating nonlinear regression for all kinetic models with experimental fitting would improve parameter accuracy and mechanistic understanding. Advanced techniques, such as surface characterization and competitive adsorption, could provide deeper insight into the structure–activity relationships of biosorbents for practical wastewater treatment applications.

REFERENCES:

1) Afolalu, S. A., Ikumapayi, O. M., Ogedengbe, T. S., Kazeem, R. A., & Ogundipe, A. T. (2022). Waste pollution, wastewater and effluent treatment methods–an overview. *Materials Today: Proceedings*, *62*, 3282-3288.
2) Chapra, S. C., Camacho, L. A., & McBride, G. B. (2021). Impact of global warming on dissolved oxygen and BOD assimilative capacity of the world's rivers: modeling analysis. *Water*, *13*(17), 2408.
3) Tella, T. A., Festus, B., Olaoluwa, T. D., & Oladapo, A. S. (2025). Water and wastewater treatment in developed and developing countries: Present experience and future plans. In *Smart Nanomaterials for Environmental Applications* (pp. 351-385). Elsevier.
4) Singh, P. K., Kumar, U., Kumar, I., Dwivedi, A., Singh, P., Mishra, S., ... & Sharma, R. K. (2024). Critical review on toxic contaminants in surface water ecosystem: sources, monitoring, and its impact on human health. *Environmental Science and Pollution Research*, *31*(45), 56428-56462.
5) Varriale, L., & Ulber, R. (2023). Fungal-Based Biorefinery: From Renewable Resources to Organic Acids. *ChemBioEng Reviews*, *10*(3), 272-292.

6) Kaur, N., Panesar, P. S., & Ahluwalia, S. (2022). Production of organic acids from agro-industrial waste and their industrial utilization. In *Valorization of Agro-Industrial Byproducts* (pp. 227-264). CRC Press.
7) Zheng, C., Zhao, L., Zhou, X., Fu, Z., & Li, A. (2013). Treatment technologies for organic wastewater. In *Water treatment*. IntechOpen.
8) El-Shamy, A. M. (2020). A review on: biocidal activity of some chemical structures and their role in mitigation of microbial corrosion. *Egyptian Journal of Chemistry*, *63*(12), 5251-5267.
9) Ebelegi, A. N., Ayawei, N., & Wankasi, D. (2020). Interpretation of adsorption thermodynamics and kinetics. *Open Journal of Physical Chemistry*, *10*(3), 166-182.
10) Liang, T., Elmaadawy, K., Liu, B., Hu, J., Hou, H., & Yang, J. (2021). Anaerobic fermentation of waste activated sludge for volatile fatty acid production: recent updates of pretreatment methods and the potential effect of humic and nutrients substances. *Process Safety and Environmental Protection*, *145*, 321-339.
11) El Messaoudi, N., Georgin, J., Ciğeroğlu, Z., Şenol, Z. M., Kazan-Kaya, E. S., Arslan, D. Ş., ... & Lacherai, A. (2024). Advanced Physicochemical Techniques for Wastewater Treatment. In *Innovative and Hybrid Technologies for Wastewater Treatment and Recycling* (pp. 37-77). CRC Press.
12) Fernandes, J., Ramísio, P. J., & Puga, H. (2024). A comprehensive review on various phases of wastewater technologies: Trends and future perspectives. *Eng*, *5*(4), 2633-2661.
13) Crini, G., & Lichtfouse, E. (2019). Advantages and disadvantages of techniques used for wastewater treatment. *Environmental chemistry letters*, *17*(1), 145-155.
14) Meka, U., Kumar, J. A., & Sivamani, S. (2025). Carbon nanomaterials from cassava rhizome for efficient toluene removal from aqueous solutions: Continuous adsorption studies using local and global optimization. *South African Journal of Chemical Engineering*.
15) Deivasigamani, P., Gajendiran, V., Chitra, B., Kumar, P. S., Balasubramanian, N., Sundararaman, S., ... & Rangasamy, G. (2025). Magnetic Nanoparticles: Synthesis, characterization and application based on environmental Perspective. *Results in Chemistry*, 102023.
16) Wu, H., Wei, H., Yang, X., Jin, C., Sun, W., Deng, K., ... & Sun, C. (2023). Spherical activated carbons derived from resin-microspheres for the adsorption of acetic acid. *Journal of Environmental Chemical Engineering*, *11*(2), 109394.
17) Hsu, C. F., Chen, Y. T., & Tseng, C. H. (2024). The performance of Adsorbing and Removing gaseous acetic acid by activate carbon. In *E3S Web of Conferences* (Vol. 530, p. 04002). EDP Sciences.
18) Zabanoot, A. A. M. M., Qatan, A. W. A. S., Hubais, A. S. M., Said, K. H. M. B., & Sivamani, S. (2023). Rejected Lime as Soil Conditioner for Growth of Vigna radiata: A Case Study from Mountainous Ranges of Dhofar Governorate, Oman. *Pakistan Journal of Agricultural Research*, *36*(4), 304-310.
19) Sivamani, S., Nazar, N. A., Krishnan, R. N., & Prasad, B. N. Biogas Production in Dhofar of Oman: Proposed Business Models and SWOT Analysis for Entrepreneurs.
20) Prasad, N., Namdeti, R., Baburao, G., Al-Kathiri, D. S. M. S., Meka, U. R., Tabook, K. M. A., & Joaquin, A. A. (2024). Central composite design for the removal of copper by an Adansonia digitata. *Desalination and Water Treatment*, *317*, 100164.

21) Al-Amri, L., Banerjee, S., Fatima, N., Ramani, S., Vijayasundaram, A., & Sivamani, S (2025). Baobab tree: A review on historical development, ecological importance, cultural significance, and economic potential. *GRS Journal of Multidisciplinary Research and Studies*, *2(4)*, 12-20.
22) Malik, V., Saya, L., Gautam, D., Sachdeva, S., Dheer, N., Arya, D. K., ... & Hooda, S. (2022). Review on adsorptive removal of metal ions and dyes from wastewater using tamarind-based bio-composites. *Polymer Bulletin*, *79*(11), 9267-9302.
23) Gajendiran, V., Deivasigamani, P., Sivamani, S., & Sivakumar, P. M. (2023). A review on cassava residues as adsorbents for removal of organic and inorganic contaminants in water and wastewater. *Journal of Chemistry*, *2023*(1), 7891518.
24) Zabanoot, A. A. M. M., Al Amri, F. M. S. I., Al Hamir, H. N. B., Al Hadhri, L. M. A., Al Abd Al-Hadhrami, M. Y., & Sivamani, S. (2025). Adsorption of Hexavalent Chromium on Raw and Activated Cassava Rhizome: Kinetic Analysis Using Mechanistic and Empirical (Regression and ANN) Models. *International Journal of Chemical Kinetics*, *57*(12), 733-743.
25) Qiu, H., Lv, L., Pan, B. C., Zhang, Q. J., Zhang, W. M., & Zhang, Q. X. (2009). Critical review in adsorption kinetic models. *Journal of Zhejiang University-Science A*, *10*(5), 716-724.
26) Musah, M., Azeh, Y., Mathew, J., Umar, M., Abdulhamid, Z., & Muhammad, A. (2022). Adsorption kinetics and isotherm models: a review. *Caliphate Journal of Science and Technology*, *4*(1), 20-26.
27) Revellame, E. D., Fortela, D. L., Sharp, W., Hernandez, R., & Zappi, M. E. (2020). Adsorption kinetic modeling using pseudo-first order and pseudo-second order rate laws: A review. *Cleaner Engineering and Technology*, *1*, 100032.
28) Hu, Q., Pang, S., & Wang, D. (2022). In-depth insights into mathematical characteristics, selection criteria and common mistakes of adsorption kinetic models: A critical review. *Separation & Purification Reviews*, *51*(3), 281-299.
29) Vareda, J. P. (2023). On validity, physical meaning, mechanism insights and regression of adsorption kinetic models. *Journal of Molecular Liquids*, *376*, 121416.
30) Benjelloun, M., Miyah, Y., Evrendilek, G. A., Zerrouq, F., & Lairini, S. (2021). Recent advances in adsorption kinetic models: their application to dye types. *Arabian Journal of Chemistry*, *14*(4), 103031.
31) Özcan, O., İnci, İ., & Aşçi, Y. S. (2013). Multiwall carbon nanotube for adsorption of acetic acid. *Journal of Chemical & Engineering Data*, *58*(3), 583-587.
32) Cruz, A. J., Pires, J., Carvalho, A. P., & Brotas de Carvalho, M. (2004). Adsorption of acetic acid by activated carbons, zeolites, and other adsorbent materials related with the preventive conservation of lead objects in museum showcases. *Journal of Chemical & Engineering Data*, *49*(3), 725-731.
33) Kannan, N., & Xavier, A. (2001). New composite mixed adsorbents for the removal of acetic acid by adsorption from aqueous solutions-a comparative study. *Toxicological & Environmental Chemistry*, *79*(1-2), 95-107.
34) Zhang, H., Lan, X., Bai, P., & Guo, X. (2016). Adsorptive removal of acetic acid from water with metal-organic frameworks. *Chemical Engineering Research and Design*, *111*, 127-137.

35) Zhang, H., Wang, Y., Bai, P., Guo, X., & Ni, X. (2016). Adsorptive separation of acetic acid from dilute aqueous solutions: adsorption kinetic, isotherms, and thermodynamic studies. *Journal of Chemical & Engineering Data*, *61*(1), 213-219.
36) Anasthas, H.M. and Gaikar, V.G., 2001. Adsorption of acetic acid on ion-exchange resins in non-aqueous conditions. Reactive and Functional Polymers, 47(1), pp.23-35.
37) Picaud, S., Hoang, P.N.M., Peybernès, N., Le Calvé, S. and Mirabel, P., 2005. Adsorption of acetic acid on ice: Experiments and molecular dynamics simulations. The Journal of chemical physics, 122(19).
38) Dina, D., Ntieche, A., Ndi, J. and Ketcha Mbadcam, J., 2012. Adsorption of acetic acid onto activated carbons obtained from maize cobs by chemical activation with zinc chloride (ZnCl2). Research Journal of Chemical Sciences, 2231, p.606X.
39) Hofman, M.S., Scoullos, E.V., Robbins, J.P., Ezeonu, L., Potapenko, D.V., Yang, X., Podkolzin, S.G. and Koel, B.E., 2020. Acetic acid adsorption and reactions on Ni (110). Langmuir, 36(30), pp.8705-8715.
40) Gomes, G.J., Zalazar, M.F., Lindino, C.A., Scremin, F.R., Bittencourt, P.R., Costa, M.B. and Peruchena, N.M., 2017. Adsorption of acetic acid and methanol on H-Beta zeolite: an experimental and theoretical study. Microporous and Mesoporous Materials, 252, pp.17-28.
41) Saha, R. K., Paula, H., Hashem, M. A., & Hira, J. (2024). Investigation of Dye Adsorption on Thermally Activated Adsorbent Derived from Tamarindus Indica Leaves. *Journal of Engineering Science*, *15*(2), 105-112.
42) Sharmin, Nowrose & Samota, Sharmila & Karim, Rezaul & Mofiz, Syed. (2025). Sustainable Wastewater Treatment using Mahogany and Tamarind-Based Bio-Coagulants and Biochar.
43) Jeppsson, L., Anehus, R., & Fredholm, D. (1999). The optimal acetate buffered acetic acid technique for extracting phosphatic fossils. *Journal of Paleontology*, *73*(5), 964-972.
44) Mattsson, A., & Osterlund, L. (2010). Adsorption and photoinduced decomposition of acetone and acetic acid on anatase, brookite, and rutile TiO2 nanoparticles. *The Journal of Physical Chemistry C*, *114*(33), 14121-14132.
45) Al-Musawi, T. J., Brouers, F., & Zarrabi, M. (2017). Kinetic modeling of antibiotic adsorption onto different nanomaterials using the Brouers–Sotolongo fractal equation. *Environmental Science and Pollution Research*, *24*(4), 4048-4057.
46) Selmi, T., Seffen, M., Sammouda, H., Mathieu, S., Jagiello, J., Celzard, A., & Fierro, V. (2018). Physical meaning of the parameters used in fractal kinetic and generalised adsorption models of Brouers–Sotolongo. *Adsorption*, *24*(1), 11-27.
47) Ibekwe, A. M., & Murinda, S. E. (2019). Linking microbial community composition in treated wastewater with water quality in distribution systems and subsequent health effects. *Microorganisms*, *7*(12), 660.
48) Yetilmezsoy, K., Demirel, S., & Vanderbei, R. J. (2009). Response surface modeling of Pb (II) removal from aqueous solution by Pistacia vera L.: Box–Behnken experimental design. *Journal of hazardous materials*, *171*(1-3), 551-562.
49) Maran, J. P., Manikandan, S., Thirugnanasambandham, K., Nivetha, C. V., & Dinesh, R. (2013). Box–Behnken design based statistical modeling for ultrasound-assisted extraction of corn silk polysaccharide. *Carbohydrate polymers*, *92*(1), 604-611.